Capillary muscle

Caroline Cohen[a,b], Timothée Mouterde[a,b], David Quéré[a,b], and Christophe Clanet[a,b,1]

[a]Laboratoire d'Hydrodynamique de l'X, UMR 7646 du CNRS, École Polytechnique, 91128 Palaiseau, France; and [b]Physique et Mécanique des Milieux Hétérogènes, UMR 7636 du CNRS, École Supérieure de Physique et de Chimie Industrielles, 75005 Paris, France

Edited by David A. Weitz, Harvard University, Cambridge, MA, and approved March 6, 2015 (received for review October 8, 2014)

The contraction of a muscle generates a force that decreases when increasing the contraction velocity. This "hyperbolic" force–velocity relationship has been known since the seminal work of A. V. Hill in 1938 [Hill AV (1938) *Proc R Soc Lond B Biol Sci* 126(843):136–195]. Hill's heuristic equation is still used, and the sliding-filament theory for the sarcomere [Huxley H, Hanson J (1954) *Nature* 173 (4412):973–976; Huxley AF, Niedergerke R (1954) *Nature* 173 (4412):971–973] suggested how its different parameters can be related to the molecular origin of the force generator [Huxley AF (1957) *Prog Biophys Biophys Chem* 7:255–318; Deshcherevskiĭ VI (1968) *Biofizika* 13(5):928–935]. Here, we develop a capillary analog of the sarcomere obeying Hill's equation and discuss its analogy with muscles.

muscle contraction | capillary analog | force–velocity relation | sliding filament | actomyosin cycle

From 1487 to 1516, Leonardo da Vinci planned to write a treatise on human anatomy. The book never appeared, but many drawings and writings have been conserved, mainly at the royal collection at Windsor (1):

> After a demonstration of all of the parts of the limbs of man and other animals you will represent the proper method of action of these limbs, that is, in rising after lying down, in moving, running and jumping in various attitudes, in lifting and carrying heavy weights, in throwing things to a distance and in swimming and in every act you will show which limbs and which muscles are the causes of the said actions and especially in the play of the arms. (2, 3)

Apart from Leonardo's attempts, the understanding of muscle contraction has been a long quest since antiquity and the work of Hippocrates of Cos (4). The topological structure of muscles was described in the anatomical studies by Andreas Vesalius in 1543 (5) and the static force generated was quantified in the first biomechanics treatise of Giovanni Borelli in 1680 (Fig. 1*A*) (6). One realizes the difficulties associated with the understanding of the force generation mechanism by comparing the scale at which the force is used (typically the body scale: 1 m) to the scale at which the force is generated [contraction of the myosin molecule: 10 nm (7)]. Eight orders of magnitude separate the molecular origin of the force from its macroscopic function, namely the motion of organisms. Considering the scales involved, research on muscles has progressed with the development of new techniques, from early microscopy for the micrometer-scale sarcomere (8), to X-ray diffraction (9) and interference microscopy (10) for the actin–myosin sliding structure, and optical tweezers for the study of individual myosin molecules (7).

Despite the complexity of the muscular system, the relation between the force F needed to move a given load and the velocity v of the motion is accessible via macroscopic experiments such as the one from Wilkie sketched in Fig. 1*B* (11). Here, a constant force $F=Mg$ is imposed by the weight E, and one records the maximal speed of contraction, $v(F)$. Decoupling inertial effects from muscle properties, one gets human muscle characteristics as shown in Fig. 1*C*. The force reaches its maximum F_0 at $v=0$, and it vanishes at a maximal speed $v=v_{max}$. The evolution between these two limits is captured by an equation proposed by Hill in 1938 (12), $(F+a)(v+b)=(F_0+a)b$, which can be written under the hyperbolic form:

$$\frac{F}{F_0}=\frac{1-v/v_{max}}{1+(F_0/a)\,v/v_{max}}. \qquad [1]$$

This equation is drawn with a solid line in Fig. 1*C* for two subjects (D.W. and L.M. in ref. 11), using the values $F_0=196$ N, $v_{max}=bF_0/a=7.5$ m/s, and $F_0/a=5$ for D.W., and $F_0=200$ N, $v_{max}=7.0$ m/s, and $F_0/a=2.1$ for L.M. The isometric tension F_0 defines the force against which the muscle neither shortens nor lengthens, and v_{max} is the maximal speed reached without load ($F=0$). These results illustrate the accuracy of Hill's equation and the variability of the parameter F_0/a between different subjects. Apart from skeletal human muscles, Hill's equation (Eq. **1**) is found to apply to almost all muscle types and over various species (13).

The contractile muscular machinery is made of parallel muscle cells that extend from one tendon to another, which connect to bones. A muscle cell is composed of nuclei and myofibrils, a linear assembly of sarcomeres, the elementary contractile unit. The typical size of sarcomeres is 3 μm, so that their number in myofibril of a 30-cm muscle cell is on the order of 10^5. A sarcomere itself is made of thin actin filaments connected to thick myosin filaments via myosin heads (Fig. 2 *C1* and *C2*). When a neuron stimulates a muscle cell, an action potential sweeps over the plasma membrane of the muscle cell. The action potential releases internal stores of calcium that flow through the muscle cell and trigger a contraction (*C2*). Actin and myosin filaments are juxtaposed but cannot interact in the absence of calcium (relaxed-state *C1*). With calcium, the myosin-binding sites are open on the actin filaments, and ATP makes the myosin motors crawl along the actin, resulting in a contraction of the muscle fiber (*C2*) (14, 15). The interaction energy increases with the number of cross-bridges, namely with the surface between actin and myosin threads.

Significance

The force generated by a muscle decreases when its contraction velocity increases. This rheology follows the heuristic Hill's equation. Here, we design and study a capillary analog in which the myosin–actin interaction is replaced by the wetting affinity between a Newtonian silicone oil and a steel rod. This device contracts and generates a force that also decreases with increasing contraction speed, following the same Hill's equation. The physical origin of this attractive equation is discussed together with the analogy between the actin–myosin system and the capillary one. Apart from its academic interest, this capillary muscle can also have extensions in technology to produce forces and motion using surface chemical energies.

Author contributions: C. Cohen, T.M., D.Q., and C. Clanet designed research, performed research, analyzed data, and wrote the paper.

The authors declare no conflict of interest.

This article is a PNAS Direct Submission.

[1]To whom correspondence should be addressed. Email: clanet@ladhyx.polytechnique.fr.

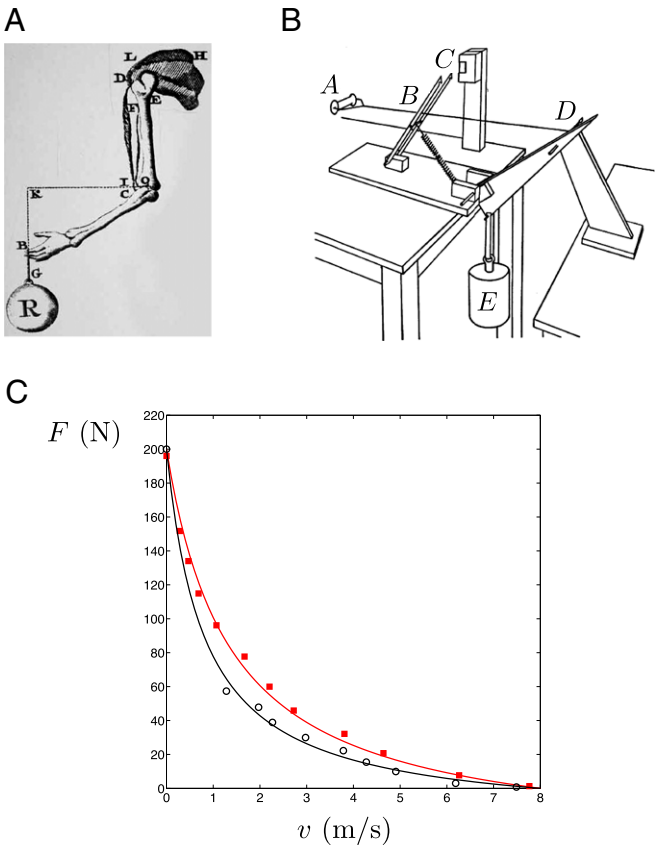

Fig. 1. (*A*) Plate of Borelli's *De Motu Animalium*. Figure courtesy of ref. 6. (*B*) Isotonic lever for human subjects [from Wilkie (11)]. A, hand grip attached to cable; B, catch to hold lever up at the end of movement; C, fixed contact; D, lever with moving contact; E, weight. (*C*) Force–velocity results obtained with two different subjects: red squares, D.W.; black circles, L.M. The solid lines are Eq. **1**, with $F_0 = 196$ N, $v_{max} = b.F_0/a = 7.5$ m/s, and $F_0/a = 5$ for D. W., and $F_0 = 200$ N, $v_{max} = 7.0$ m/s, and $F_0/a = 2.1$ for L.M. (data from ref. 11).

Hill's equation is a heuristic law and its connection to the sliding-filament model has first been established via adjustable correlations (16) and later via strong theoretical assumptions (17). The purpose of the present article is to build a capillary analog of the sliding-filament model, to record the corresponding force–velocity relationship, and to show how this minimal model system leads to Hill's equation.

Capillary Muscle: Setup and Results

Our device is sketched in Fig. 2 *A* and *B*. A cylindrical glass tube (length, $L = 10$ cm; diameter, $2R = 5$ mm) filled with a Newtonian silicone oil (density, $\rho = 950$ kg/m^3; viscosity, $\eta = 0.1$–1 Pa·s; surface tension, $\gamma = 0.022$ N/m) lies on polystyrene floating on a water bath, a setup chosen to minimize friction. Once in contact with a rigid fixed steel wire (diameter, $2r = 1.8$ mm), the glass tube moves to encompass and wet the wire. Because the glass tube is equipped with a trailing hook, it entrains at $t = 0$ and $x = -x_0$ a vertical glass fiber on which it exerts a force F (Fig. 2*B*). We denote $x(t)$ as the hook position. We initially have $x = -x_0$, and for $x \geq 0$ the hook location corresponds to the deflection of the fiber from its initial vertical position.

An example of a capillary contraction is presented in Fig. 2*D*, where oil has a viscosity $\eta = 1$ Pa·s. As soon as the contact is established between the solid rod and the wetting liquid in the tube (top image), a capillary force $F_0 \approx 100$ μN attracts the tube, which moves to the right. The "capillary muscle" contracts and it generates a force as soon as the hook meets the vertical fiber. The time indicated on each picture reveals a nonlinear contraction. We have achieved contractions for two different x_0, 7.6 and 36 mm. Both contractions lead to the same equilibrium state $x_{max} \approx 38$ mm but with different dynamics, as shown on Fig. 3*B*.

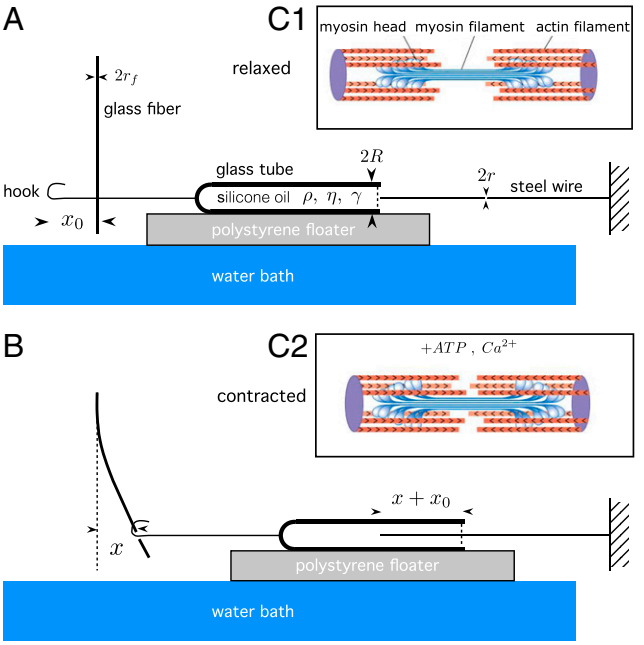

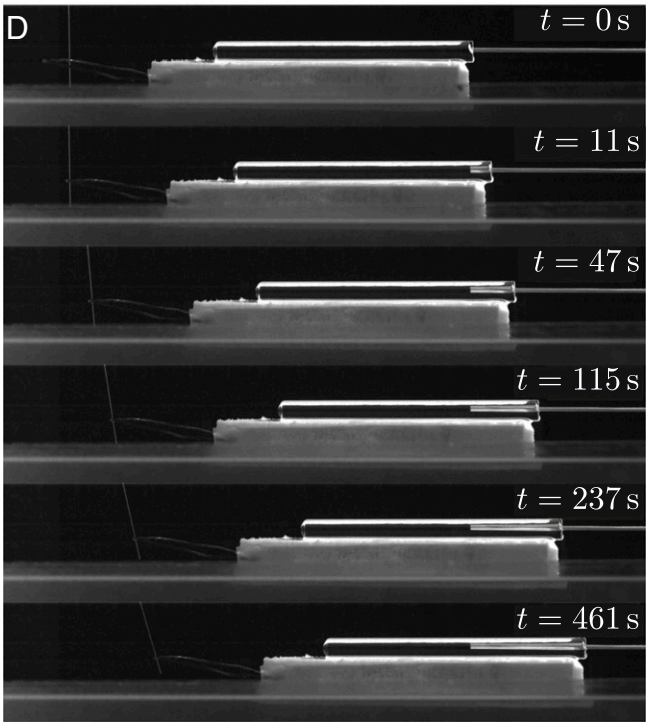

Fig. 2. Experimental setup of a capillary muscle and its biological inspiration, the sarcomere. The steel wire is equivalent to the myosin filament that slides in the silicone oil tube, which stands for the actin filament. (*A*) Position at $t = 0$, corresponding to relaxed state of the sarcomere (*C1*). (*B*) Position at $t > 0$, corresponding to the contracted state of the sarcomere (*C2*). (*D*) Example of capillary contraction obtained with $2r = 1.8$ mm, $2R = 5$ mm, $\eta = 1$ Pa·s, $\gamma = 22$ mN/m, $k = 3.3$ μN/m, and $x_0 = 7.6$ mm.

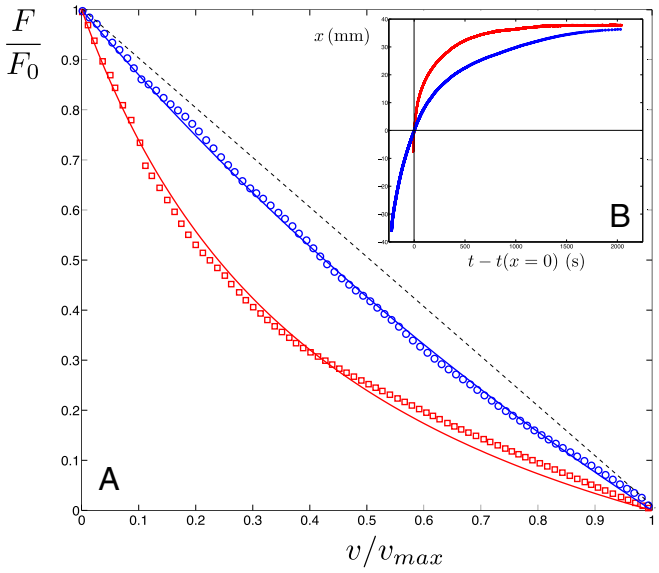

Fig. 3. (*A*) Normalized force F/F_0 as a function of the reduced velocity of contraction v/v_{max} obtained with the oil used in Fig. 2*D* and two initial values of $x_0 = 7.6$ mm (red squares) and $x_0 = 36$ mm (blue circles). The solid lines are the best fits obtained with Hill's equation (Eq. **1**) using $F_0/a = 0.34$ (blue circles) and $F_0/a = 2.17$ (red). The inset (*B*) shows the dynamics of capillary contraction in these two experiments.

We extract from the deflection $x(t)$ both the force $F(t) = kx(t)$ and the velocity $v = dx/dt$. The relation $F(v)$ between the force and the velocity is displayed in Fig. 3 for the two values of x_0 (7.6 mm in red squares, and 36 mm in blue circles). This figure reveals that F decreases as the velocity v increases in a way reminiscent of the one observed with muscles (Fig. 1*C*).

Capillary Muscle: Model

In the above experiment, the capillary driving force is $F_0 = 2\pi r\gamma$, whereas the resisting forces are the elastic force F related to the elastic glass fiber, the viscous friction F_η in the glass tube, and the inertia F_i of the floating tube. Using the values from Fig. 2*D*, we get $F_0 \approx 100$ μN. In that experiment, the mass of the compound (filled tube plus floater) is $M = 15$ g. Using G for the characteristic acceleration, we evaluate in Fig. 2*D* the inertia term $F_i = MG$ to 0.1 μN because $G \approx 10^{-5}$ m/s^2. Newton's law, $F_i = F_0 - F - F_\eta(v)$, thus reduces to the quasi-steady limit, $F = F_0 - F_\eta$.

Elastic Force, *F*. The deflection of a thin elastic rod (diameter, $2r_f$; length, L_f) under the action of a localized force F is a classical problem since Euler's elastica (18). In the small slope limit, the elastica predicts a linear relationship between the force F and the deflection x_{max} of the fiber as follows:

$$F = k\,x_{max} \quad \text{with} \quad k = \frac{3EI}{L_f^3}, \qquad [2]$$

where E and I stand for Young's modulus and moment of inertia, respectively. For a cylindrical glass fiber, $E = 64$ GPa and $I = \pi r_f^4/4$. We tested the linearity of Eq. **2** using wetting liquids of low viscosity, to reduce the time to reach equilibrium. Because the applied force $F = 2\pi r\gamma$ depends on both the radius r of the steel wire (Fig. 2) and on surface tension, we varied both parameters to increase the range of loads. For each experiment, once the contact between the wire and the wetting liquid is established, we wait for equilibrium and measure the final fiber deflection x_{max}. The relation $F(x_{max})$ is indeed found to be linear, as shown in Fig. 4*A*, from which we deduce a stiffness $k = 3.3$ μN/mm. With $r_f = 120$ μm and $L_f = 21$ cm, the value expected from Eq. **2** is 3.4 μN/mm, in good agreement with the experiment.

Viscous Force, F_η. Without glass fiber, Fig. 4*B* shows that the tube moves along the steel wire with a diffusive type of dynamics: $(x+x_0)^2 \sim t$, as soon as the wire contacts the liquid in the tube $[x(t=0) = -x_0]$. Even if there is no fiber here, we still use the notation $x + x_0$ to be consistent with the conventions defined in Fig. 2. This distance simply represents the wetted length along the steel wire (*Inset* in Fig. 4*B*).

As for Washburn's imbibition (19, 20), the diffusive-like behavior results from a balance between a constant driving force $(2\pi r\gamma)$ and a viscous resisting force, $\alpha\eta v 2\pi(x+x_0)/\ln(R/r)$. In this latter expression, $v = d(x+x_0)/dt$ and α is a coefficient

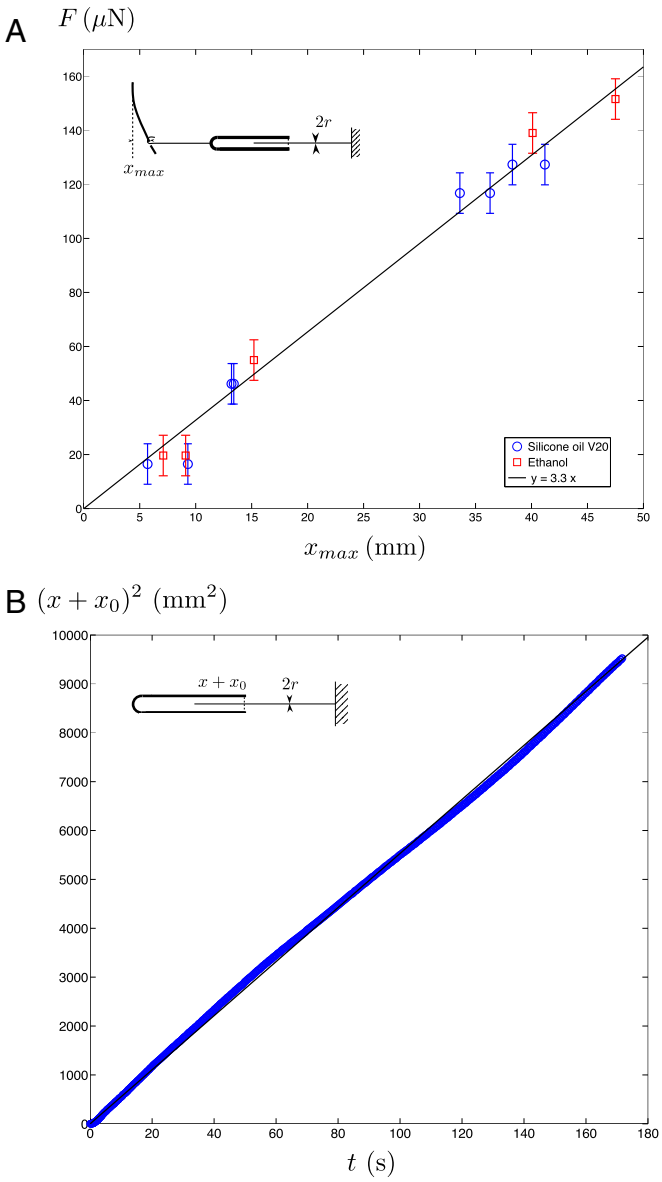

Fig. 4. (*A*) Relationship between the maximal deflection of the fiber x_{max} and the applied force $F = 2\pi r\gamma$. *Inset* is a sketch of the experiment. (*B*) Time evolution of the square of the wetted distance $x + x_0$ for $2r = 1.8$ mm and silicone oil V1000 ($\eta = 1$ Pa·s and $\gamma = 0.022$ N/m).

accounting for the exact structure of the velocity profile in the tube ($\alpha = 1$ when the tube is centered). This balance yields the following:

$$(x + x_0)^2 = \frac{2\gamma r}{\alpha\eta} \ln\left(\frac{R}{r}\right) t. \quad [3]$$

Using $R = 2.5$ mm, $\gamma = 0.022$ N/m, and $\eta = 1$ Pa·s, we get from the fit (thin solid line) in Fig. 4*B*: $\alpha \approx 0.72$.

Hill's Equation for a Capillary Muscle. The quasi-steady equilibrium $F = F_0 - 2\pi\alpha\eta v(F/k + x_0)/\ln(R/r)$ can be rewritten as follows:

$$\frac{F}{F_0} = \frac{1 - v/v_{max}}{1 + (F_0/a)\, v/v_{max}}, \quad [4]$$

with $F_0 = 2\pi r\gamma$, $F_0/a = 2\pi r\gamma/kx_0$, and $v_{max} = F_0 \ln(R/r)/2\pi\alpha\eta x_0$. This equation is identical to Hill's equation (Eq. **1**). The solid lines in Fig. 3 correspond to hyperbolic fits obtained with Eq. **4** and $F_0/a = 2.17$ (red squares) and $F_0/a = 0.34$ (blue circles). Since $F_0 = 2\pi r\gamma$ and k have not been changed, $F_0/a = F_0/k.x_0$ should vary as $1/x_0$. This is indeed what we measure because $2.17/0.34 \approx 36/7.6$. The larger x_0, the smaller F_0/a and the closer we get to the asymptotic linear behavior $F/F_0 = 1 - v/v_{max}$ expected for $F_0/a = 0$.

The Sliding-Filament Model and Its Capillary Analog

Capillary Analog. Analogies between liquids and tissues have led to valuable findings in the context of embryonic mutual envelopment (21) or tissue spreading (22). Steinberg showed that embryonic tissues may behave like liquids and can be characterized by a well-defined surface tension (23). This analogy lately extended to the spreading dynamics of cellular aggregates (24, 25). Here, we pursue this kind of analogy to illustrate the myosin–actin interaction in a muscle. The muscle contraction results from the actin–myosin interactions. Each myosin head can be in two different states, attached to the actin filament or detached from the actin filament. We denote $\Delta\mathcal{E}_{head} = \mathcal{E}_{attached} - \mathcal{E}_{detached}$ as the difference of energy of a myosin head between these two states. This energy is negative once calcium is supplied, thus leading to actomyosin binding, and it remains positive without calcium. When a myosin head binds to actin, it induces an energy variation $\Delta\mathcal{E}_{head}$ and it occupies a surface $S_0 \sim l^2$, where l is the typical size of the myosin head. This implies an equivalent surface energy $\gamma_{eq} = -\Delta\mathcal{E}_{head}/S_0$, analogous to the estimation of a liquid surface tension kT/a^2, where kT is a typical van der Waals cohesion energy and a^2 is a molecular surface area (20). The total energy involved in a thick filament can then be expressed as follows:

$$\Delta\mathcal{E} = \frac{\Delta\mathcal{E}_{head}}{S_0} S = -\gamma_{eq} S, \quad [5]$$

where S/S_0 is the total number of myosin heads (and S is the attachable surface area). Because $-\Delta\mathcal{E}_{head}$ is the typical energy released during ATP hydrolysis (30 kJ/mol) and because the head of myosin is around 10 nm, one gets $\gamma_{eq} \approx 0.5$ mN/m.

Our capillary device can be seen as a physical analog of the myosin/actin system, as sketched in Fig. 2: the solid rod ("myosin") slides in a wetting liquid ("actin"). As the myosin rod penetrates the actin tube by a distance $x + x_0$, its energy varies by an amount $\Delta\mathcal{E} = 2\pi r(x + x_0)(\gamma_{sl} - \gamma_{sv})$, where γ_{sl} and γ_{sv} stand for solid–liquid and solid–vapor surface tension, respectively. Using Young's equation, we get $\Delta\mathcal{E} = -\gamma \cos\theta\, 2\pi r(x + x_0)$, where θ is the contact angle and γ is the liquid–vapor surface tension (26). The wetting limit ($\cos\theta > 0$) corresponds to the "calcium" state

Fig. 6. Example of capillary relaxation obtained for a superhydrophobic wire initially forced into a tube filled with water: The tube moves so as to expel the wire.

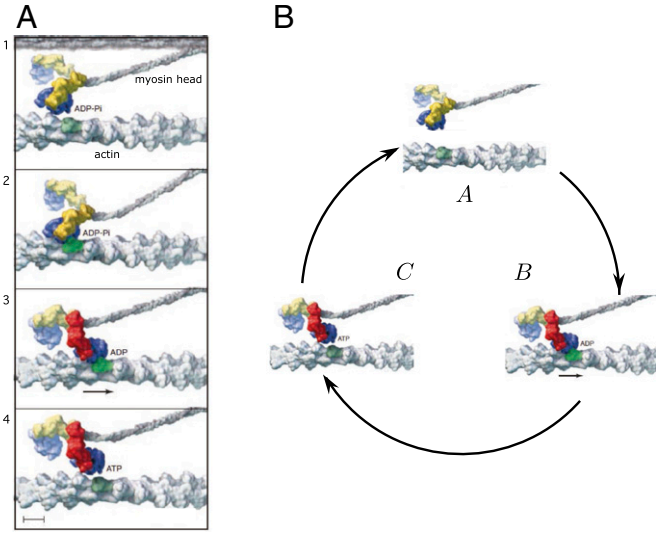

Fig. 5. (*A*) Model for the motility cycle of muscle myosin extracted from ref. 36. (Scale bar in frame 4: 6 nm.) Myosin is a dimer of two identical motor heads (catalytic cores are blue; lever arms in the prestroke ADP-Pi state are yellow) anchored to the thick filament (*Top*) by a coil (gray rod extending to the *Upper Right*). In the ADP-Pi bound state, the catalytic core weakly binds to actin. Frame 2: One head docks properly onto an actin binding site (green). The two heads act independently, and only one attaches to actin at a time. Frame 3: Actin docking causes phosphate release from the active site. The lever arm then swings to the poststroke, ADP-bound state (red), which moves the actin filament by 10 nm. Frame 4: After completing the stroke, ADP dissociates and ATP binds to the active site, which rapidly reverts the catalytic core to its weak-binding state. The lever arm recocks back to its prestroke state (i.e., back to frame 1). (*B*) Cycle of attachment A–force generation B–detachment C.

where penetration in the actin bundle is favored, whereas the nonwetting limit $\cos\theta < 0$ corresponds to the no-calcium state. For $\theta = 0$, we simply have the following:

$$\Delta\mathcal{E} = -\gamma S, \quad [6]$$

where $S = 2\pi r(x + x_0)$ is the wetted surface area of the "myosin" rod. This expression is identical to Eq. **5**. The liquid viscosity leads to dissipation and it mimics the energy consumption of the muscle, which we now discuss together with its link with Hill's equation.

Sliding Filament and Hill's Equation. According to Needham (4), "the first hints of the sliding-filament mechanism of contraction were given by the low-angle X-ray diffraction patterns obtained by H. E. Huxley with living and glycerol-extracted muscle" (27). A theory for the contraction based on this sliding-filament model was then proposed by A. F. Huxley in 1957 (16), where different parameters were chosen to approach Hill's equation. In 1968, Deshcherevskii (17) proposed to derive Hill's equation using some assumptions on the sliding-filament model. We present the main steps of this model and then establish the connection with capillary muscles.

In the sliding-filament model, the force is generated by myosin heads connecting myosin to thin actin filaments (Fig. 2*C*). This scenario has been confirmed since refs. 28 and 29, and we summarize the force cycle in Fig. 5*A*. In the absence of ATP, myosin heads are attached to actin. Although this state is very short in living muscle, it is responsible for muscle stiffness in death. As binding ATP, myosin heads release from actin filaments, which requires energy.

Deshcherevskii considered three main stages for the force cycle (Fig. 5*B*). A myosin head is either "free" (A), or developing an active force (B), or detaching (with a breaking force) (C). Each head moves from one state to another one following the sequence A–B–C–A. Denoting n and m as the number of myosin heads in the states B and C and α_D as the total number of myosin heads in one-half a sarcomere, Deshcherevskii expresses the rate of change of both populations as follows:

$$\frac{dn}{dt} = k_1.[\alpha_D - (n+m)] - \frac{v}{l}n, \quad [7]$$

$$\frac{dm}{dt} = \frac{v}{l}n - k_2.m, \quad [8]$$

where k_1 is the constant rate for the transition from state A to B, and k_2 is the constant rate of opening bridges leading to a transition from C to A; l is the mean value of conformational transformation of the myosin head during the power stroke ($l \approx 10$ nm). Because v is the velocity of relative displacement of the threads, the ratio l/v is the time after which one active head switches from being stretched (active) to compressed (resisting). In the steady regime where v is a constant, the populations of the three stages A, B, and C remain constant on average and one deduces $vn/l = k_1\ (\alpha_D - (n+m))$ and $vn/l = k_2 m$. Different groups have worked on actomyosin interactions outside sarcomere. Assuming that the active and breaking forces developed by the myosin head are identical and equal to f, found to be on the order of 3 pN (7, 30–33), the force developed by a sarcomere is $F = f\ (n-m)$. Using the above expressions for n and m, we directly get Eq. **1** with $F_0 = \alpha_D.f$, $F_0/a = 1 + k_2/k_1$, and $v_{max} = k_2.l$.

Identification with Eq. **4** provides some insight about the analogy between sliding filaments and capillary muscles. As expected from the previous section, the maximal force $F_0 = 2\pi r\gamma$ in Eq. **4** corresponds to the force $\alpha_D f$ developed by all myosin heads. The force ratio $F_0/a = 2\pi r\gamma/kx_0$ in Eq. **4** is found here to be only a function of the reaction rates $1 + k_2/k_1$. Changing the hook location x_0 is thus a way to vary the ratio between the reaction rates of the two transitions A–B and C–A. Finally, the maximal velocity v_{max} of the capillary muscle is reached when the hook first contacts the vertical fiber, that is, for $F_0 = 2\pi\alpha\eta v_{max}x_0/\ln(R/r)$. The velocity v_{max} is reached when $n = m$, that is, when the inactivation rate v_{max}/l equals the detaching rate k_2. Hence the viscosity allows us to tune the reaction rate of the transition C–A.

Inverted Capillary Motion. Our capillary device was found to generate a contractile force analogous to that of a real muscle. From a practical point of view, it is worth exploring the possibility of inducing a reverse motion. To do so, we inverted the wettability by treating the steel wire with a hydrophobic colloidal suspension (Glaco; Soft99). After drying the solvent, the fiber was observed to be superhydrophobic (advancing and receding angles of $171 \pm 3°$ and $164 \pm 3°$). Starting from a configuration where the fiber is immersed in a tube filled with water, we observe in Fig. 6 that the motion indeed takes place in the reverse direction (compared with Fig. 2*D*) to minimize the contact between the liquid and the wire. This behavior is reminiscent of the transition from contraction to relaxation (*C2–C1* transition in Fig. 2). If the device is let free, the wire gets eventually expelled from the tube. This experiment also shows that a system of tunable wettability [by means of temperature or light (34)] should be able to successively generate contraction and relaxation.

Conclusion and Perspectives

We have designed a minimal capillary model of force generator following Hill's contraction law. The model is based on three main characteristics, which exist both in muscles and in its capillary analog:

i) Inertia is not involved and the system contracts in a quasi-steady regime.
ii) The force driving the contraction is based on surface affinity between two surfaces that can slide with respect to each other.
iii) The device not only generates a force but also dissipates energy.

It was often proposed, in the biomechanics community, that Hill's equation can be recovered with a spring-dashpot macroscopic model involving a non-Newtonian dissipation (13). Here, we showed that a Newtonian fluid also allows to recover the hyperbolic force–velocity relation, provided one accounts for the sliding structure of the contraction, which induces a nonlinear term "xv" in the dissipation, which is necessary to get Hill's equation. The analogy might be pursued to understand other systems, such as living single cells, which have been lately found to also follow Hill's equation (35).

Finally, a capillary muscle can be discussed in terms of innovation. We have shown that tuning the contact angle allows the cell either to contract or to relax. As in real muscles, this elementary contractile unit can be coupled to other identical contractile units, in series or parallel to increase the contraction speed or the force generated. Microfluidics and robotics are possible areas of application.

1. Keele KD (1979) *Corpus of the Anatomical Works in the Collection of Her Majesty the Queen* (Johnson, New York).
2. O'Malley CD, Saunders JB (1982) *Leonardo da Vinci on the Human Body* (Gramercy Books, New York).
3. Keele KD (1983) *Leonardo da Vinci's Elements of the Science of Man* (Academic, New York).
4. Needham DM (1971) *Machina Carnis: The Biochemistry of Muscular Contraction in its Historical Development* (Cambridge Univ Press, Cambridge, UK).

5. Vesalius A (1543) *De Humani Corporis Fabrica*; trans Garrison DH, Hast MH (2003) [*On the Fabric of the Human Body*] (Northwestern University, Evanston, IL).
6. Borelli GA (1680) *De Motu Animalium*; (Ex Typographia Angeli Barnabo, Rome).
7. Finer JT, Simmons RM, Spudich JA (1994) Single myosin molecule mechanics: Piconewton forces and nanometre steps. *Nature* 368(6467):113–119.
8. Bowman W (1840) On the minute structure and movements of voluntary muscle. *Philos Trans R Soc Lond Biol* 130:457–501.
9. Huxley H, Hanson J (1954) Changes in the cross-striations of muscle during contraction and stretch and their structural interpretation. *Nature* 173(4412):973–976.
10. Huxley AF, Niedergerke R (1954) Structural changes in muscle during contraction; interference microscopy of living muscle fibres. *Nature* 173(4412):971–973.
11. Wilkie DR (1949) The relation between force and velocity in human muscle. *J Physiol* 110(3-4):249–280.
12. Hill AV (1938) The heat of shortening and the dynamic constants of muscle. *Proc R Soc Lond B Biol Sci* 126(843):136–195.
13. McMahon TA (1984) *Muscles, Reflexes, and Locomotion* (Princeton Univ Press, Princeton).
14. Huxley AF (1974) Muscular contraction. *J Physiol* 243(1):1–43.
15. Huxley HE (2004) Fifty years of muscle and the sliding filament hypothesis. *Eur J Biochem* 271(8):1403–1415.
16. Huxley AF (1957) Muscle structure and theories of contraction. *Prog Biophys Biophys Chem* 7:255–318.
17. Deshcherevskiĭ VI (1968) [Two models of muscle contraction]. *Biofizika* 13(5):928–935. Russian.
18. Landau LD, Lifshitz EM (1959) *Theory of Elasticity* (Pergamon, Oxford).
19. Washburn EW (1921) The dynamics of capillary flow. *Phys Rev* 17(3):273–283.
20. De Gennes P-G, Brochard-Wyart F, Quéré D (2003) *Capillarity and Wetting Phenomena: Drops, Bubbles, Pearls, Waves* (Springer, New York).
21. Foty RA, Pfleger CM, Forgacs G, Steinberg MS (1996) Surface tensions of embryonic tissues predict their mutual envelopment behavior. *Development* 122(5):1611–1620.
22. Ryan PL, Foty RA, Kohn J, Steinberg MS (2001) Tissue spreading on implantable substrates is a competitive outcome of cell-cell vs. cell-substratum adhesivity. *Proc Natl Acad Sci USA* 98(8):4323–4327.
23. Manning ML, Foty RA, Steinberg MS, Schoetz EM (2010) Coaction of intercellular adhesion and cortical tension specifies tissue surface tension. *Proc Natl Acad Sci USA* 107(28):12517–12522.
24. Douezan S, et al. (2011) Spreading dynamics and wetting transition of cellular aggregates. *Proc Natl Acad Sci USA* 108(18):7315–7320.
25. Douezan S, Brochard-Wyart F (2012) Spreading dynamics of cellular aggregates confined to adhesive bands. *Eur Phys J E Soft Matter* 35(11):116.
26. de Gennes P-G (1985) Wetting: Statics and dynamics. *Rev Mod Phys* 57(3):827–863.
27. Huxley HE (1953) X-ray analysis and the problem of muscle. *Proc R Soc Lond B Biol Sci* 141(902):59–62.
28. Rayment I, et al. (1993) Structure of the actin-myosin complex and its implications for muscle contraction. *Science* 261(5117):58–65.
29. Huxley HE (1996) A personal view of muscle and motility mechanisms. *Annu Rev Physiol* 58(1):1–19.
30. Molloy JE, Burns JE, Kendrick-Jones J, Tregear RT, White DCS (1995) Movement and force produced by a single myosin head. *Nature* 378(6553):209–212.
31. Gebhardt JCM, Clemen AEM, Jaud J, Rief M (2006) Myosin-V is a mechanical ratchet. *Proc Natl Acad Sci USA* 103(23):8680–8685.
32. Sellers JR, Veigel C (2010) Direct observation of the myosin-va power stroke and its reversal. *Nat Struct Mol Biol* 17(5):590–595.
33. Thoresen T, Lenz M, Gardel ML (2011) Reconstitution of contractile actomyosin bundles. *Biophys J* 100(11):2698–2705.
34. Feng XJ, Jiang L (2006) Design and creation of superwetting/antiwetting surfaces. *Adv Mater* 18(23):3063–3078.
35. Mitrossilis D, et al. (2009) Single-cell response to stiffness exhibits muscle-like behavior. *Proc Natl Acad Sci USA* 106(43):18243–18248.
36. Vale RD, Milligan RA (2000) The way things move: Looking under the hood of molecular motor proteins. *Science* 288(5463):88–95.